

Structured doping with light forces

Th. Schulze, T. Mütter, D. Jürgens, B. Brezger, M. K. Oberthaler,^{a)} T. Pfau,^{b)} and J. Mlynek

Fachbereich Physik and Optik-Zentrum, Universität Konstanz, D-78457 Konstanz, Germany

(Received 11 October 2000; accepted for publication 22 January 2001)

Light forces are a powerful tool for neutral atom manipulation and have been used previously to focus an atomic beam onto a substrate to create periodic nanostructures. We utilize the material-selective characteristic of the atom–light interaction to structure the material composition of a film during growth. A host and a dopant material are evaporated simultaneously, but only the dopant is focused by the light field. The dopant concentration varies laterally on a sub-100-nm-length scale. This technique can be extended to three-dimensional patterning and opens up ways to engineer the photonic, electronic, or magnetic features of a solid. © 2001 American Institute of Physics. [DOI: 10.1063/1.1355664]

Laser sources and a detailed understanding of the atom–light interaction have been used to cool and trap atoms¹ and to realize a great variety of optical elements for neutral atoms² such as atom mirrors, beam splitters, or wave guides. A lithography technique based on standing light fields acting as atomic lens arrays has been developed and periodic nanostructures in one³ and two⁴ dimensions have been produced. The action of the lens array on the atomic beam relies on the resonantly enhanced induced dipole force. Because atom lenses exploit the resonance condition, they are highly material selective. This feature was used in our experiment to focus one atomic species out of a two-component beam. A film is grown on a substrate placed in the focal plane of the lens array. The chemical composition of the film is laterally structured in a simple one-step process.

For the first experimental realization of structured doping with light forces, we use chromium as a dopant and magnesium fluoride as a host material. The chromium beam and magnesium fluoride beam are generated with two independent high-temperature effusion cells ($T_{\text{Cr}}=1650^\circ\text{C}$, $T_{\text{MgF}_2}=1400^\circ\text{C}$). Its divergence is reduced to below 0.5 mrad by laser cooling¹ of the transverse degrees of freedom. The well-collimated atomic beam impinges on the lens array made of light, as sketched in Fig. 1. It is realized by retro-reflecting a laser beam to form a standing light wave.⁵ The laser frequency is tuned 40 natural linewidths above the chromium transition ${}^7S_3 \rightarrow {}^7P_4$ at $\lambda=425.6$ nm (natural linewidth 5 MHz).

The light field induces an oscillating electrical dipole moment in the chromium atoms, which is resonantly enhanced. A conservative force arises from the interaction of the induced dipole with the local laser electric field. It deflects the atoms towards the nodes of the standing light wave, which thus acts as an array of cylindrical lenses with a period of $\lambda/2=213$ nm. A substrate is placed in the focal plane of these lenses and the chromium atoms are deposited in a line pattern with this period. Simultaneously, magnesium fluoride

is evaporated onto the same substrate. It is a standard dielectric coating material whose refractive index depends on the chromium doping concentration. Thus, periodic doping with chromium leads to a photonic crystal for visible wavelengths.

During deposition through a light mask, magnesium fluoride experiences only negligible light forces because there is no resonant enhancement, and is thus deposited homogeneously. The chemical composition of the resulting film, therefore, is spatially modulated, corresponding to the chromium pattern (see Fig. 1). The dopant concentration is structured laterally with a period of $\lambda/2=213$ nm and does not vary along the growth direction.

The picture described so far does not take into account the effect of the growth process on the dopant distribution, e.g., diffusion could smear out the doping structure. Since this cannot be predicted theoretically, only an experiment could prove the feasibility of the proposed method for structured doping. In our experiment, we evaporated magnesium fluoride and chromium for 15 min, leading to a film thickness of 40 ± 5 and 20 ± 5 nm, respectively. This high chromium concentration was chosen in order to get a clear chromium signal for the microanalysis.

The material composition of the grown film was analyzed on a nanometer scale by two different techniques. With

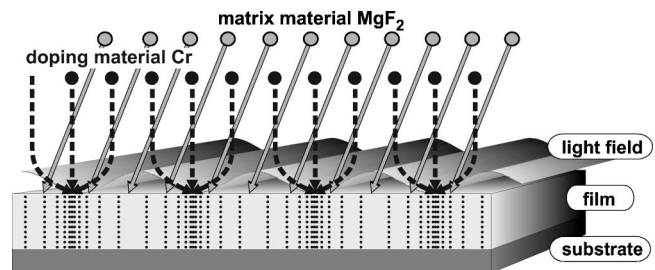


FIG. 1. Sketch of the principle of structured doping with light forces. Two materials, in our experiment chromium and magnesium fluoride, are evaporated on a substrate simultaneously. With a standing light wave, one of the materials is addressed using the element specific atom–light interaction. In the experiment the magnesium fluoride serves as host while the chromium transition ${}^7S_3 \rightarrow {}^7P_4$ at $\lambda=425.6$ nm is used to focus the dopant chromium atoms on a sub-100-nm-length scale with a period of $\lambda/2=213$ nm.

^{a)}Electronic mail: markus.oberthaler@uni-konstanz.de

^{b)}Also at: 5.Physikalisches Institut, Universität Stuttgart, D-70550 Stuttgart, Germany.

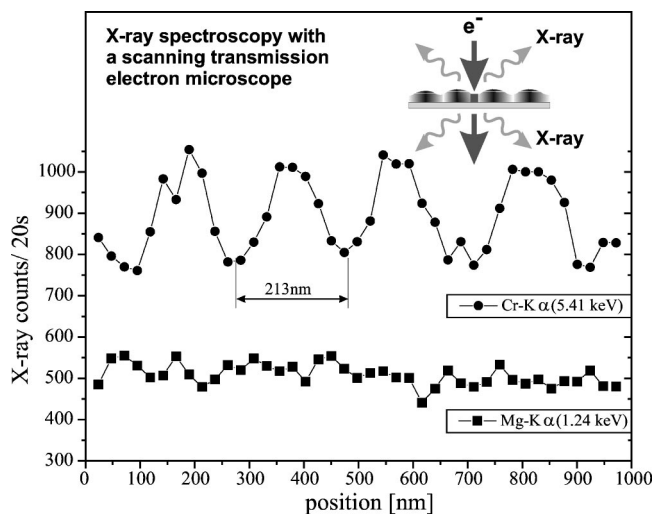


FIG. 2. Lateral material composition of the film was analyzed by scanning an electron beam over the film and detecting the characteristic x-ray emission (see the inset). The graph shows the x-ray counts at the energies 5.41 keV ($\text{Cr } K\alpha$) and 1.24 keV ($\text{Mg } K\alpha$) over the position perpendicular to the lines. The light field addresses the chromium atoms and, therefore, only the chromium composition is modulated periodically whereas the magnesium fluoride concentration is constant. The deviation of the pattern from periodicity can be attributed to drifts during the scan.

a scanning transmission electron microscope (STEM) in combination with energy-dispersive x-ray spectrometry (EDX),⁶ we analyzed the lateral material composition averaged through the film. High spatial resolution Auger electron spectroscopy (AES) (Ref. 7) allowed us to determine the material composition in the growth and lateral directions.

The STEM/EDX measurements⁸ only achieve high lateral resolution for thin samples. Therefore, we used as a substrate a 20 nm Formvar® film on a TEM Ni-support grid. During a field scan with the fast scan axis parallel to the lines, the x-ray counts at the energies 5.41 keV ($\text{Cr } K\alpha$) and 1.24 keV ($\text{Mg } K\alpha$) were integrated over 20 s for each point. Figure 2 shows the count rates at the $\text{Cr } K\alpha$ and the $\text{Mg } K\alpha$ energies as a function of the beam position perpendicular to the lines with a resolution of 25 nm. The magnesium concentration is constant whereas the chromium concentration varies periodically with the period of $\lambda/2 = 213$ nm. These results confirm the creation of a pattern that is not washed out due to lateral diffusion effects. As the signal is integrated through the whole film, it also proves that during the growth the drift of the substrate with respect to the light field was much smaller than the pattern period.

In order to determine the material composition in the growth direction, another sample was analyzed with a scanning electron microscope (SEM) and the Auger electrons were used as a surface sensitive probe with less than 5 nm penetration depth. This sample was grown under identical conditions on a silicon substrate with a homogeneous ~ 5 nm chromium adhesion layer. Auger electron spectra,⁹ laterally averaged over several pattern periods, were taken at depths of 4, 10, 20, and 50 nm by sputtering material away. In the spectra shown in Fig. 3(a), the peaks can be assigned to the corresponding elements as indicated. The relative magnitudes of the chromium, the fluoride, and the magnesium peaks, i.e., the ratios of their concentrations, are equal in the second and third spectra. The oxygen peak is attributed to

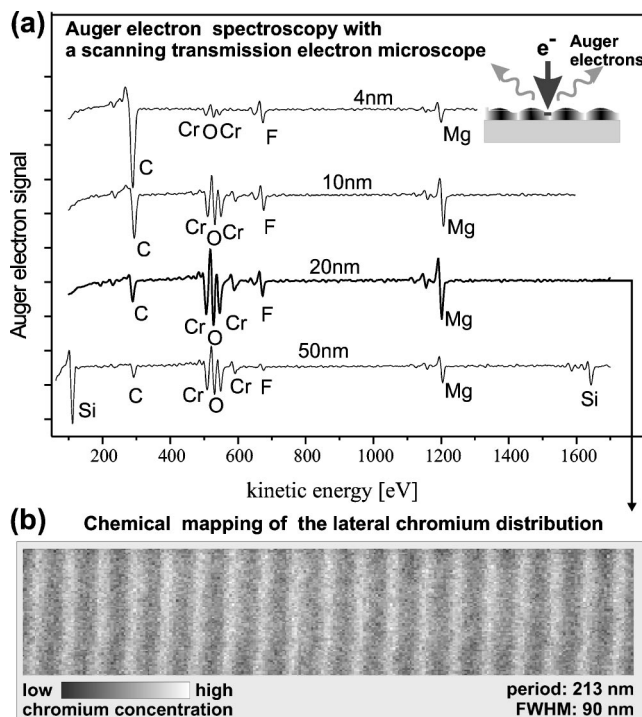


FIG. 3. Material composition of a thin layer can be measured by scanning an electron beam and using the Auger electrons as a surface sensitive probe (see the inset). Depth information is obtained by *in situ* sputtering between data acquisition. (a) Auger electron spectra performed after four different depths of 4, 10, 20, and 50 nm, showing the material composition averaged laterally over $3 \times 4 \mu\text{m}^2$. The spectra reveal that the relative concentration of chromium, fluorine, and magnesium within the film is constant. (b) Very-high resolution spatial mapping of the chromium concentration after sputtering 20 nm into the film. The calibration of the length scale due to the known light field period of $\lambda/2 = 213$ nm gives a chromium concentration FWHM of 90 nm.

oxidation of the chromium during growth (vacuum in the growth chamber around 5×10^{-6} mbar). The carbon peak which dominates the uppermost spectrum and diminishes with sputtering depth is attributed to surface contamination and indiffusion from the carbon pad used to fix the sample during transport and analysis. After 50 nm sputtering the spectrum shows mainly the silicon substrate and the chromium adhesion layer. This is in good agreement with the film height deduced from the quartz-rate monitors. A very high-resolution mapping⁹ (20 nm spot size) of the lateral chromium distribution is deduced from the Auger electron signal at a depth of 20 nm [Fig. 3(b)]. After calibrating the length scale due to the known light field period of $\lambda/2 = 213$ nm, the full width at half maximum (FWHM) of the chromium concentration is measured to be 90 nm.

Additional patterning along the growth direction can be readily accomplished in various ways and extends the method to three-dimensional doping. A method commonly applied in thin-film technology and molecular-beam epitaxy is flux control of the different components [Fig. 4(a)]. Utilizing specific properties of atom manipulation with light, one can change the lateral pattern by switching the intensities [Fig. 4(b)],¹⁰ frequencies, or polarizations¹¹ of the laser beams constituting the light field. Since the light field can be continuously varied during the deposition process, more general structures in three dimensions than with previously dem-

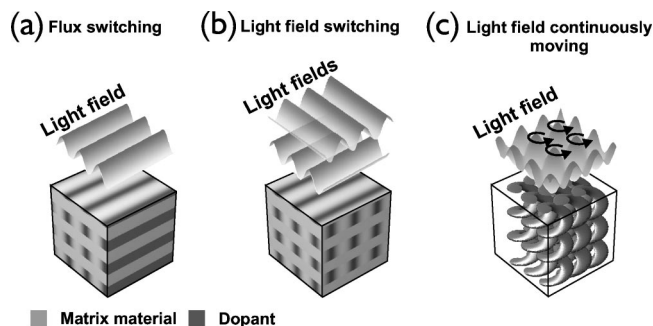


FIG. 4. Different dopant structures realizable with the demonstrated method of structured doping with light forces. (a) Switching the flux of the dopant. (b) Two standing light fields can be switched alternately to create structures known from photonic band-gap materials (see Ref. 13). (c) The versatility of light manipulation is best demonstrated by the possibility to continuously change the lateral structure during growth, e.g., circularly moving the light field.

onstrated methods are possible, e.g., periodic chiral structures [Fig. 4(c)].

Since doping a material generally changes its physical properties, e.g., refractive index, the presented method is a way of producing engineered nanoscale structures like photonic crystals.¹² There the spatial modulation of the refractive index can lead to photonic band gaps, i.e., light of a certain frequency cannot propagate inside the structure. In order to estimate our refractive index modulation, we produced a MgF₂ film with a macroscopic chromium concentration gradient. The refractive index as a function of chromium concentration was determined with standard ellipsometry. This allows us to deduce a refractive index modulation of 0.2 for the realized films with periodic chromium concentration (see Fig. 2). This is too small for a photonic band gap. Applying the method to other dopant materials allows us to increase the modulation of the refractive index. Combining our nonintrusive and clean method with molecular-beam epitaxy could revolutionize the field of material engineering. Optical focusing of the technologically interesting group III atoms¹³ would allow the modification of the band-gap energy of a III–V semiconductor in three dimensions. This opens up the way to creating complex three-dimensional electronic potentials, e.g., channel-like three-dimensional conductor networks.

In this letter, we present a technique for structured doping on the sub-100 nm scale during the growth process. The

technique relies on the material-selective property of the atom–light interaction, which allows us to address one atomic species in a multicomponent beam. In this experiment we used a single standing light wave to create a line pattern. More complex patterns and smaller periods in one and two dimensions have already been achieved by light forces acting on a single-component atomic beam.^{4,11} This opens up ways to generate very general three-dimensional structures.

The authors wish to thank Professor Dr. R. Wurstler for performing the STEM/EDX measurements and Dr. E. Nold for doing the SEM/AES measurements. One of the authors (Th.S.) acknowledges a fellowship from the Carl–Zeiss–Schott Förderstiftung. This work was supported by the Deutsche Forschungsgemeinschaft (Grant SFB 513), the Optik–Zentrum Konstanz, and the TMR–network “Nanofab.”

¹J. Glanz, *Science* **278**, 578 (1997); C. S. Adams and E. Riis, *Prog. Quantum Electron.* **21**, 1 (1997).

²C. S. Adams, M. Sigel, and J. Mlynek, *Phys. Rep.* **240**, 143 (1994).

³G. Timp, R. E. Behringer, D. M. Tennant, J. E. Cunningham, M. Prentiss, and K. K. Berggren, *Phys. Rev. Lett.* **69**, 1636 (1992); J. J. McClelland, R. E. Scholten, E. C. Palm, and R. J. Celotta, *Science* **262**, 877 (1993).

⁴R. Gupta, J. J. McClelland, Z. J. Jabbour, and R. J. Celotta, *Appl. Phys. Lett.* **67**, 1378 (1995); U. Drodofsky, J. Stuhler, Th. Schulze, M. Drewsen, B. Brezger, T. Pfau, and J. Mlynek, *Appl. Phys. B: Lasers Opt.* **65**, 755 (1997); B. Brezger, Th. Schulze, P. O. Schmidt, R. Mertens, T. Pfau, and J. Mlynek, *Europhys. Lett.* **46**, 148 (1999).

⁵A Gaussian laser beam with a waist of 100 μm and a power of 20 mW is used. In the direction along the atomic beam, this Gaussian profile is cut in the center by the substrate.

⁶J. Goldstein, *Scanning Electron Microscopy and X-Ray Microanalysis* (Plenum, New York, 1992).

⁷C. L. Hedberg, *Handbook of Auger Electron Spectroscopy* (Physical Electronics, Eden Prairie, MN, 1995).

⁸These measurements have been performed with a high-resolution scanning electron microscope (ABT DS 150F, Topcon, Tokyo) in cooperation with Professor Dr. R. Wurstler at the Institut für Physik, Universität Hohenheim.

⁹These measurements have been performed with a high-performance scanning Auger electron spectrometer (Perkin–Elmer F-Sonde 680) by Dr. E. Nold at the Institut für Materialforschung, Forschungszentrum Karlsruhe.

¹⁰S. Y. Lin, J. G. Fleming, D. L. Hetherington, B. K. Smith, R. Biswas, K. M. Ho, M. M. Sigalas, W. Zubrzycki, S. R. Kurtz, and J. Bur, *Nature (London)* **394**, 251 (1998).

¹¹Th. Schulze, B. Brezger, P. O. Schmidt, R. Mertens, A. S. Bell, T. Pfau, and J. Mlynek, *Microelectron. Eng.* **46**, 105 (1999); Th. Schulze, B. Brezger, R. Mertens, M. Pivk, T. Pfau, and J. Mlynek, *Appl. Phys. B: Lasers Opt.* **70**, 671 (2000).

¹²J. D. Joannopoulos, P. R. Villeneuve, and S. Fan, *Nature (London)* **386**, 143 (1997).

¹³S. J. Rehse, R. W. McGowan, and S. A. Lee, *Appl. Phys. B: Lasers Opt.* **70**, 657 (2000).